Late Holocene changes in vegetation and fire within a forest refuge in the Araripe region, northeastern Brazil

Maria Daniely Freire Guerra, Marie-Pierre Ledru, Sergio Augusto Santos Xavier, Rudney de Almeida Santos, Francisca Soares de Araújo

Paper to be submitted to The Holocene

Late Holocene changes in vegetation and fire within a forest refuge in the Araripe region, northeastern Brazil

Maria Daniely Freire Guerra[1], Marie-Pierre Ledru[2*], Sergio Augusto Xavier[2,3], Rudney de Almeida Santos[2,3], Francisca Soares de Araújo[3]

[1] Geosciences Department, Regional University of Cariri, Coronel Antônio Luiz St., Pimenta, Crato-CE, 63105-000, Brazil

2 Institut des Sciences de l'Evolution de Montpellier (ISEM), Université de Montpellier-CNRS-IRD-EPHE, 34095 Montpellier cedex 05, France

3 Programa de Pós-Graduação em Ecologia e Recursos Naturais, Departamento de Biologia, Campus do Pici, Universidade Federal do Ceará, Fortaleza- 60455-760, CE, Brazil

*corresponding author

Email: marie-pierre.ledru@ird.fr

Abstract

In semi-arid northeastern Brazil, where water is scarce, rainforest refugia can be seen along the coastal relief, where the trade winds bring in humidity from the Atlantic Ocean, or further inland, at the Araripe plateau where water comes from aquifer resurgence. In order to reconstruct past changes in water resurgence and in their associated vegetation types, we analyzed pollen, charcoal and trace elements from sediment cores collected in the permanent swamps created by the resurgences. Our high temporal resolution analyses show that the vegetation was more sparse and drier than today until 2700 cal yr BP. Between 2700 and 2000 cal yr BP, palm swamp and evergreen forest tree taxa started to expand, suggesting an increase in water resurgence. At 2000 cal yr BP the moist forest with *Mauritia* expanded and fire activity changed from mixed to woody fuel particles. During the last 200 cal yr BP, a decrease in the palm tree *Mauritia flexuosa*, an expansion of Poaceae and an increase in macrocharcoal particles are attributed to an increase in anthropogenic activities in the Araripe Basin. The late Holocene climatic trend seen at Araripe mirrors that of eastern Brazil and has controlled the aquifer activity, including during the major droughts that affected the region. This is highly relevant for the application of public policies that rely on the aquifers of Araripe for the 21st century.

Keywords

Cerrado, aquifer, charcoal, pollen, *Mauritia*, human impact

Introduction

As semi-arid environments are characterized by a scarcity, even the absence, of surface water, the main source for drinking water supply, agricultural, and industrial purposes, is generally represented by groundwater (Dillon et al., 2022). In the semi-arid region of north-east Brazil (NEB), located between 3°S and 16°S latitude, due to shallow and stony soils originating from impermeable rocks of the crystalline basement (Sampaio 1995), the water supply is predominantly from surface water basins (Ledru et al., 2020), except for a small region of central NEB which benefits from resurgences of water coming from the northeastern slope of Chapada do Araripe. Because of the natural dry conditions and increasing water demand, NEB is regularly confronted with water insecurity issues (Marengo et al., 2022). During the last century, NEB has experienced recurrent droughts, with dramatic effects on the environment (Marengo and Bernasconi 2015). The Araripe plateau (*Chapada do Araripe* in Portuguese) is located ~500 km from the coast in the middle of a densely populated semi-arid region exposed to the effects of climate change (Marengo et al., 2020). However, the Araripe plateau sustains a forest refuge thanks to aquifer resurgence able to supply year-round water resources (Costa et al., 2023). Due to the high permability of the soils of the plateau, the water is stored in aquifers with an exudation of perennial springs at ~700 m asl. The water of these aquifers results from a strong interaction between surface water and groundwater (Mendonça et al., 2004). What confers the perpetuity of the water flow in the exudation zones of Araripe is the residence time of the water in the suspended aquifer, which according to Mendonça (2001) is 180 years, and gradually guarantees the frequency of the outflow. However, demography, agricultural practices and the on-going temperature increase are putting a threat to this precious water resource and the Brazilian water agency estimated that the amount of groundwater extracted is much larger than the

mean annual recharge (Mendonça et al., 2004). In addition, the progressive decrease in precipitation is also impacting the mean annual recharge of the aquifer as for instance observed during the last long period of drought, from 2012 to 2016 (Costa et al., 2023). During the Holocene, speleothem-based climate reconstructions show a progressive installation of drier conditions in NEB from early to late Holocene along an east-west moisture gradient (Cruz et al., 2009; Utida et al., 2020). However, little is known about the evolution of the forest refugia during the Holocene. The pollen record from the Maranguape refugia (Montade et al., 2014), a rainforest enclave near the coast, showed a major dry episode at ~4200 yr BP followed by a progressive return of humidity, although never returning to the pre-4200 yr BP level. Albeit with variable intensity, the 4200 yr event was well observed from the west to the east of NEB (Utida et al., 2020). However, after the 4200 yr BP event, NEB was split into two climatic regions, with western NEB becoming more moist (Xavier et al., 2024) and eastern NEB becoming drier (Utida et al., 2020). Today, as the region is subject to progressive drying (Marengo and Bernasconi 2015) it is urgent to conserve the forest to preserve the water quality. To better assess the future of the aquifers of the Araripe and their associated moist forest, we collected two sediment cores near the water resurgences and performed muliproxy analyses. We reconstructed the impacts of drought and of human activity on the vegetation dynamic and biodiversity of the Araripe plateau during the last 5300 years. Finally, we discussed the future of the forest refuge in the context of on-going climate change, the increasing demand for water in the upwelling areas for domestic and agricultural consumption and, the need to manage the provision of water for the local population.

Study area

Geology

The Araripe Basin is a highland "oasis" located in the middle of a semi-arid region (Fig. 1). The residual relief of Araripe forms a plateau of 900 km² reaching an elevation of 1000 m asl (Morales and Assine, 2015), and is a unique area within the drought polygon represented by the State of Ceará (Fig. 1). It is the largest inland basin in NEB and is formed from Palaeozoic and Mesozoic continental and marine deposits. The lithostratigraphy comprises the Cariri Valley Group, with Cariri (Paleozoic), Brejo Santo (Jurassic) and Abaiara (Cretaceous) formations, and of the Araripe Group composed of Barbalha, Santana, Araripina and Exu Cretaceous formations (Assine 2007). The Araripe plateau was the first Brazilian national forest conservation unit, created in 1946 and has been included in UNESCO's Global Geoparks Network (GGN) since 2006, because of the presence of important paleontological and geological sites (Cabral and Mota, 2010; Herzog, 2017). The superposition of layers with different thicknesses, lithologies, facies and ages favored the formation of three levels of aquifers: a lower level with an average thickness of 100 m, a middle level with an average thickness of 500 m and an upper level with an average thickness of 320 m (DNPM, 1996). The upper aquifer of the Exu Formation, between 800 and 1000 m asl, is formed of fluvial sandstones with an average thickness of 320 m, situated within an exudation of perennial springs at ~700 m asl, which generate local moisture, feeding the surface hydrography and maintaining regional conditions that are in contrast to the surrounding semi-aridity (Guerra et al., 2020; 2023).

Aquifer recharge depends on annual rainfall and the time for the water to resurface varies depending on the location. On the western side of the plateau the water residence lasts ~180 years, with a mean flow of ~85 m^3/ yr (Mendonça, 2001).

Climate

The local climate (with a dry summer, according to Alvares et al., 2013) is characterized by a mean annual precipitation (MAP) of 1100 mm, concentrated between January and May, a mean annual temperature (MAT) of 24°C with little variation throughout the year and a mean average annual potential evapotranspiration of ~120 mm (Supplementary Figures 1 and 2) (SUDENE, 2021).

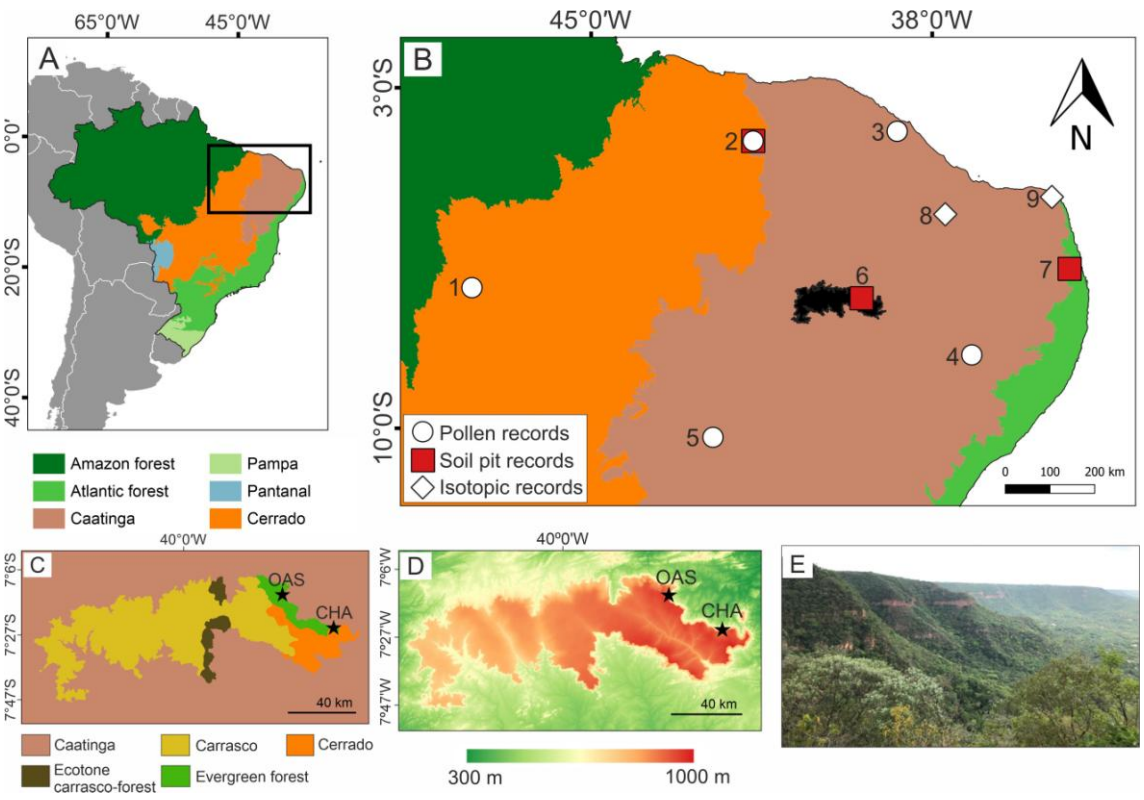

Figure 1. (A) A map of South America indicated the Brazilian biomes; (B) The location of the Araripe plateau (in black) and of the records discussed in the text: 1. Chapada das Mesas (Xavier et al., 2024); 2. Sete Cidades (Pessenda et al., 2010; Xavier et al., 2022); 3. Serra do Maranguape (Montade et al., 2014); 4. Catimbau (Moraes et al., 2020); 5. Icatu (Oliveira et al., 1999); 6. Araripe National Forest (Pessenda et al., 2010); 7. Guaribas Reserve (Pessenda et al., 2010); 8. Apodi cave (Utida et al., 2020); 9. Lake Boqueirão (Utida et al., 2019). (C) A map of the Araripe plateau showing the distribution of vegetation and the location of the cores OAS-20

and CHA-20. (D) A topographical map of the Araripe plateau with the location of the cores OAS-20 and CHA-20; (E) A picture showing the northern edge of the Araripe plateau.

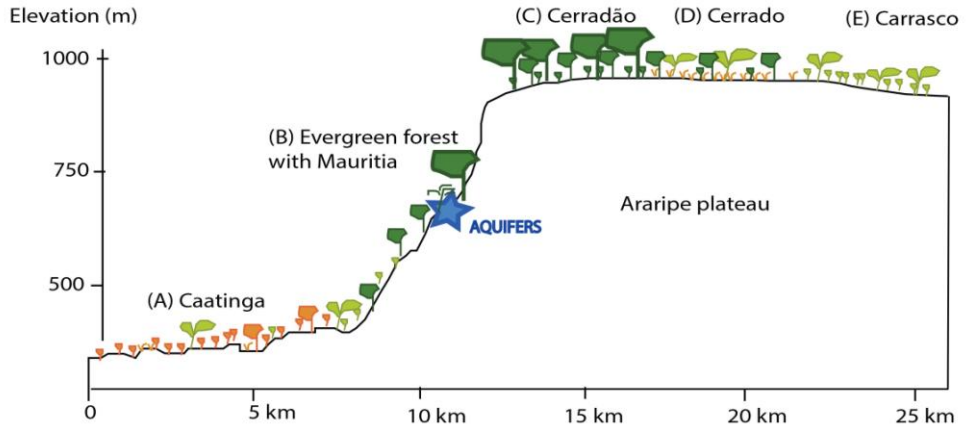

Figure 2. Schematic altitudinal profile showing the main vegetation physiognomies found between the lowlands and the summit of the Araripe plateau (from Guerra et al., 2020; Loiola et al., 2015; Pessenda et al., 2010), the location of the aquifers at ~700 m elevation (blue star) and pictures of the vegetation types observed on the plateau: (A) Caatinga (during the dry season) (B) Evergreen forest, (C) cerradão, (D) cerrado *sensu stricto* and (E) Carrasco (see text for explanation).

NEB rainfall patterns are modulated by four types of drivers that interact at different levels as a function of location (e.g., eastern NEB versus western NEB): the South American Summer Monsoon (SASM), the Inter Tropical Convergence Zone (ITCZ), cold surges activated by the temperature gradient between the southern pole and the equator, and the South Atlantic Subtropical Dipole (SASD) (Marengo and Bernasconi

2015; Marengo et al., 2012, 2018; Wainer et al., 2021). The interhemispheric sea surface temperature (SST) gradient controls the position of the ITCZ north and south of the equator in the tropical Atlantic Ocean with the ITCZ at its furthest south from March to May, when NEB experiences its rainy season during the negative phase of the SASD (Wainer et al., 2021). Abnormal rainfall seen at Araripe is also observed when moisture from the South Atlantic Ocean reaches the Araripe plateau, which is modulated by the strength of the south-east trade winds and of the Atlantic Subtropical High (Rao et al., 1993). The El Niño–Southern Oscillation Events (ENSO) can have a strong influence on the interannual variation of the regional climate (Marengo et al., 2017). The historical precipitation series for Crato and Missão Velha (Supplementary Figure 1) shows irregularities in their interannual distribution with, for example, two extreme droughts in 1919 and 1958 associated with an El Niño episode. Another driver of drought conditions is the anomalous northward position of the ITCZ during a positive phase of the SASD, when colder SSTs are observed in the Southern Atlantic (and inversely for extreme rainfall) (Andreoli and Kayano, 2006; Marengo and Bernasconi 2015).

Vegetation

The vegetation of NEB is dominated by the Caatinga phytogeographic domain (Moro et al., 2016) also known as the "drought polygon" (*Polígono das secas* in Portuguese*)*. However, the flora of the Araripe plateau is under the influence of the northeastern phytogeographic Cerrado province (Ratter et al., 2003; Moro et al., 2015). It comprises typical species from several Cerrado physiognomies (Fig. 2), such as a seasonal evergreen forest, which forms a type of headwater forest near the aquifers as a consequence of the water resurgence on the northeastern slope of the plateau, and also

133 favors frequent fogs on the top of the plateau (Loiola et al., 2015). From the moist
134 northern edge to the dry interior of the plateau, the succession of cerradão (a semi-
135 deciduous forest), cerrado sensu stricto (a semi-deciduous woody savanna with a grass
136 layer) and Carrasco (a deciduous shrubland) follows the soil moisture gradient (Guerra
137 et al., 2020). Below 400 m asl, the Caatinga, a dry deciduous forest and the most
138 characteristic vegetation of the semi-arid NEB, covers the bottom of the plateau (Fig. 2)
139 (Guerra et al., 2020; Loiola et al., 2015; Pessenda et al., 2010; Ribeiro-Silva et al.,
140 2012). In the seasonal evergreen forest, represented by both a headwater forest near the
141 OAS aquifer at 700 m asl (Benicío et al., 2023), and a semi-deciduous (cerradão) type
142 of cloud forest at the top of the plateau between 904 and 967 m asl (Santos et al., 2019),
143 the families Fabaceae, Myrtaceae and Rubiaceae present the highest number of species,
144 while *Brosinum gaudichaudii* (Moraceae), *Talisia esculenta* (Sapindaceae),
145 *Machaerium acutifolium* (Fabaceae) and *Ouratea* sp. (Ochnaceae) are among the most
146 represented species (Benício et al., 2023). Other families, such as Salicaceae,
147 Annonaceae and Chrysobalanaceae, are also well represented in both humid forest types
148 (Supplementary Table 1). In the cerradão, the families with the highest species richness
149 are represented by Myrtaceae and Fabaceae (Macêdo, 2014), while *Ocotea nitida*
150 (Lauraceae), *Protium heptaphyllum* (Burseraceae), *Licania* sp. (Chrysobalanaceae),
151 *Cordiera myrciiflora* (Rubiaceae) and *Bowdichia virgiloides* (Fabaceae) are among the
152 most abundant species. In the cerrado *sensu stricto*, at 900 m asl, Fabaceae, Myrtaceae,
153 Poaceae, Apocynaceae, Euphorbiaceae and Malpighiaceae. are the most represented
154 families, and *Protium* (Burseraceae), *Byrsonima* (Malpighiaceae) and *Solanum*
155 (Solanaceae) the most represented genera (Costa et al., 2004) (Supplementary Table 1).
156 The phytosociology of an enclave of cerrado located within the Caatinga at a low
157 elevation (200-400 m) represents a dry type of cerrado, with among others the genera

Astronium and *Curatella* represented (Calixto-Júnior et al., 2021) (Supplementary Table 1).

In the Carrasco the dominant families are Caesalpiniaceae and Lauraceae, with *Senegalia langsdorffii*, *Hymenaea eriogyne* and *Manihot caerulescens* among the most represented species (Ribeiro-Silva et al., 2012) (Supplementary Table 1). The Caatinga is represented mainly by the families Fabaceae and Euphorbiaceae (Lemos and Meguro, 2015; Loiola et al., 2015) (Supplementary Table 1).

Material and methods

Coring

Two sediment cores were collected in 2020 from the *Mauritia* swamps that today grow at the resurgence of the aquifers at ~ 700 m asl (Figures 1C and 2). The 170-cm core of Oasis Araripe (OAS-20) (7°13′52.69″S, 39°28′30.83″W, 737 m asl) was collected from the municipality of Crato, and the 130-cm core Chamu (CHA-20) (7°24’27.96”S, 39°12’10.40”W, 763m asl) from the municipality of Missão Velha (Fig. 1B), using a Russian corer. The sediment cores were transferred into PVC half-tubes and sealed in a plastic sheath for transport to the University of Montpellier, France. After performing the non-destructive analyses (X-ray Fluorescence; XRF), samples for radiocarbon dates were collected from along the cores (see below); and the cores were sliced every centimeter, and the samples kept in labelled plastic bags and stored at 4ºC.

Chronology, pollen, charcoal and XRF scanning

A total of 11 samples from core OAS-20 and seven samples from core CHA-20 were extracted for radiocarbon dating by accelerator mass spectrometry (AMS) at the French *Laboratoire de Mesure du Carbone* 14 (LMC14). The age-depth models were built

using the Bacon package (Blaauw and Christen, 2011), and ages were calibrated using the SHCal20 curve (Hogg et al., 2020).

For the macrocharcoal analyses, samples of 0.5 cm^3 taken at 2-cm intervals were prepared using bases NaOCl and KOH for bleaching and a 160-µm mesh for sieving (Stevenson and Haberle, 2005). The charcoal particles were counted and measured under a stereoscope using WinSeedle software (Regent Instruments, Quebec, Canada). The results are expressed as particles accumulation (number of particles/cm^2), surface area accumulation of CHARa (total area/cm^2/year) and the average width/length (W/L) ratio. The W/L ratio is a measure of burnt vegetation, where $W/L < 0.5$ indicates burnt grasses produced by large and intense fires in open grassland and $W/L > 0.5$ indicates burnt woody material produced by forested ecosystems (Aleman et al., 2013; Haliuc et al., 2023).

For palynological analyses, samples of 0.5 cm^3 were taken at 1-cm intervals and analyzed at 2-cm intervals using a combination of an acid-free protocol (Santos and Ledru, 2021) and standard techniques (Faegri and Iversen, 1989) to achieve better concentrations of the final residue using hydrofluoric acid when necessary to eliminate the remaining small silica particles. Two tablets of the exotic marker *Lycopodium clavatum* were added to the samples prior to chemical treatment, to calculate the pollen concentration (Stockmarr, 1971). At least 300 terrestrial pollen grains were counted, excluding aquatic and water level-related taxa. Pollen, spore and non-palynomorph percentages were calculated relative to the sum of terrestrial pollen sum. Pollen identification was carried out using the ISEM pollen reference collection, pollen atlases (Cassino and Meyer, 2011; Colinvaux et al., 1999; Escobar-Torrez et al., 2023b; Lorente et al., 2017) and an online database (Bush and Weng, 2007).

Graphics were built using Psimpoll, a pollen-diagram plotting software (Bennett, 2009), and zonation was based on hierarchical clustering using the CONISS method (Grimm, 1987).

The XRF core scanning was performed at a resolution of 0.5 cm at the *Laboratoire EDYTEM Université Savoie Mont-Blanc* – CNRS. Two runs were adjusted at 10 KV and 30 KV to measure the trace elements.

Results

Lithology

The sediment from core OAS-20 consisted of a laminated grey clay layer intercalated with sand and charcoal layers between 170 and 120 cm, and a brown organic clay layer between 120 and 20 cm. From 20 cm to the top there was a layer of vegetal fibers and roots, which was discarded. The sediment from CHA-20 consisted of fine grey organic clay intercalated with brown organic clay and black charcoal layers (Supplementary Figures 3, 4 and 5).

Chronology

The age-depth model for core OAS-20 showed a hiatus between 138 and 125 cm, with an age of 5315 cal yr BP at the base of the core (Table 1 and Fig. 3A). Pollen analyses indicated that the hiatus occurred at 128 cm (see for instance abrupt changes in *Cuphea*, *Lindernia, Casearia* on Supplementary Figure 6). Consequently, the results were considered in two parts, one for the bottom part of core OAS-20, representing the interval between 5300 and 4100 cal yr BP, and the other for the top of the core representing between 1100 and 0 cal yr BP.

The base of core CHA-20 was dated to 4100 cal yr BP, with no observable gap in sedimentation (Table 2 and Fig. 3B, Supplementary Figure 7).

Table 1. Radiocarbon dates for core OAS-20, showing ^{14}C calibrated BP ages (2σ ranges) (Hogg et al., 2020).

Lab. code	**Depth (cm)**	**$\delta^{13}C$**	**^{14}C yr BP**	**Median probability (cal yr BP)**
SacA64739	35	-26.1	20 ± 30	360
SacA67201	48	-26,6	470 ± 30	495
SacA64740	55	-24,2	610 ± 30	545
SacA67202	62	-25,7	610 ± 30	590
SacA64075	80	-20,2	750 ± 30	690
SacA61868	97	-28,7	1550 ± 30	875
SacA64741	111	-36,1	1215 ± 30	1000
SacA64076	125	-25,2	1090 ± 30	1055
SacA64742	138	-25,2	3895 ± 30	4360
SacA60349	149	-27,6	4465 ± 30	4920
SacA64077	163	-20,2	4525 ± 30	5180

240

241

242

243 **Table 2 -** Radiocarbon dates for core CHA-20, showing ^{14}C calibrated BP ages (2σ

244 ranges) (Hogg et al., 2020).

245

Lab. Code	Depth (cm)	$\delta^{13}C$	^{14}C yr BP	Median probability (cal yr BP)
SacA67984	17	-24.9	-120 ± 30	
SacA67985	43	-28,2	1670 ± 30	1525
SacA67204	60	-28,0	2375 ± 30	2345
SacA67986	93	-29,6	3435 ± 30	3640
SacA67987	108	-29,2	3350 ± 30	3530
SacA67988	121	-28,3	3785 ± 30	4110
SacA60348	124	-28,2	3640 ± 30	3915

246

247

248

A

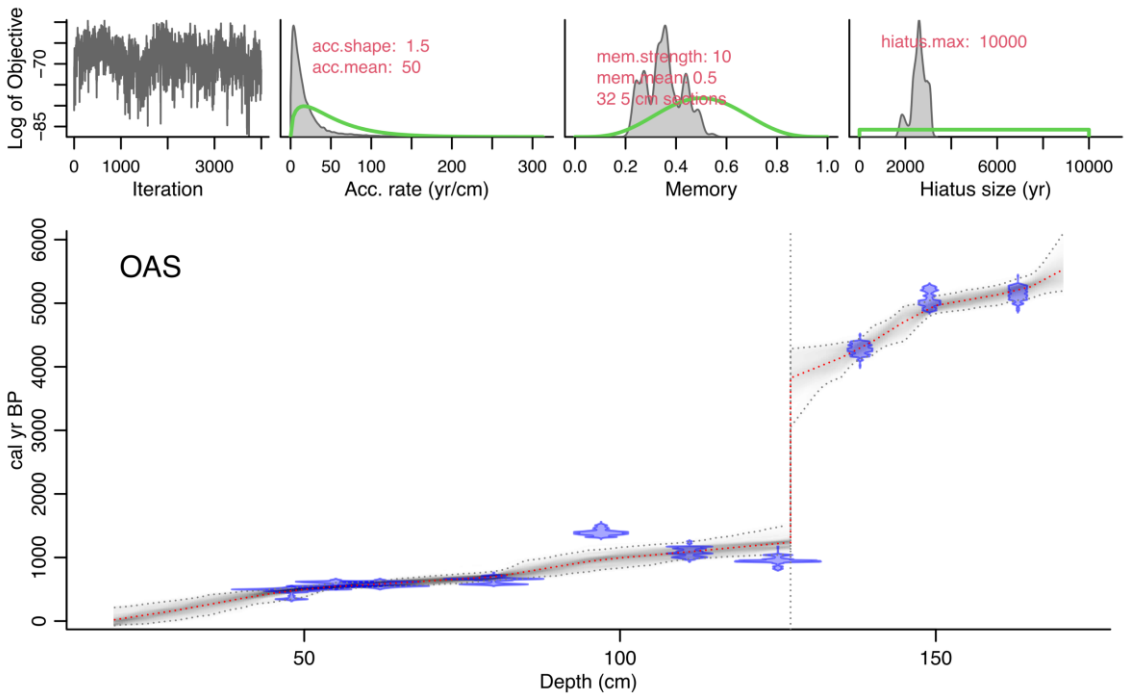
Log of Objective
Iteration
acc.shape: 1.5
acc.mean: 50
Acc. rate (yr/cm)
mem.strength: 10
mem.mean: 0.5
32.5 cm sections
Memory
hiatus.max: 10000
Hiatus size (yr)
OAS
cal yr BP
Depth (cm)

B

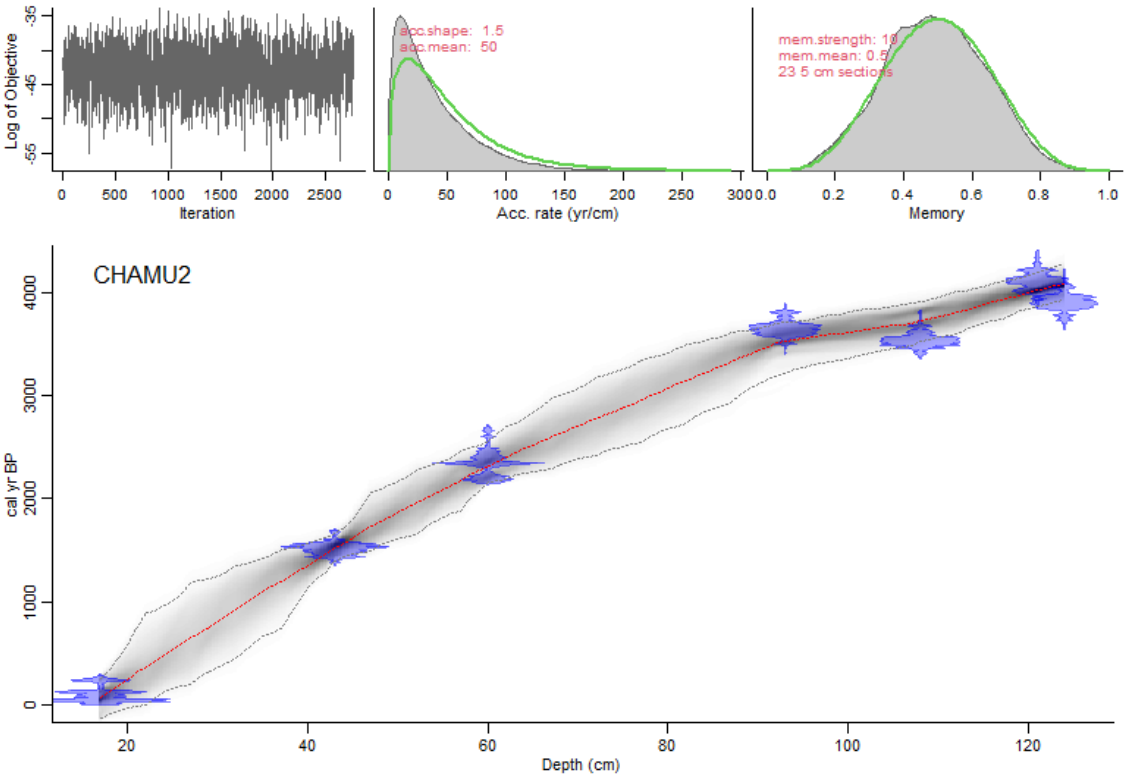
Log of Objective
Iteration
acc.shape: 1.5
acc.mean: 50
Acc. rate (yr/cm)
mem.strength: 10
mem.mean: 0.5
23.5 cm sections
Memory
CHAMU2
cal yr BP
Depth (cm)

Figure 3. A Bacon age/depth model (red dashed line) for **(A)** core OAS-20 and core **(B)** CHA-20 overlaying the calibrated distributions of the individual radiocarbon dates (blue) (see Tables 1 and 2) . Dark gray areas show the 95% confidence intervals of the models (Blaauw and Christen, 2011).

XRF analyses

The Ti/Al ratio was used to represent the terrigenous input, which is closely related to energy transport, where high values are indicators of coarse particles deposition (Arnaud et al., 2012; Lopez et al., 2006) (Figures 4 and 5, and described within the pollen zones below). Other trace elements (Fe/Zr, K/Ti, Br/Ti, Si/Al, Ti/Ca) showed the same trends as Ti/Al and are represented in Supplementary Figures 10 and 11.

Macrocharcoal analyses

For macrocharcoal analyses of core OAS-20, 74 samples distributed along 150 cm of the core were taken at 2-cm intervals between 20 and 170 cm. CHARa was smaller in the lower part of the core (5300-4200 cal yr BP, between 0 and 0.008 $mm^2/cm^2/yr$) than in the upper part (1100 to 200 cal yr BP, between 0.001 and 0.016 $mm^2/cm^2/yr$) (Fig. 4). The W/L ratio highlighted two different periods of charcoal particle presence with grass particles in the bottom section and some mixed fuel particles in the upper section (Supplementary Figure 8).

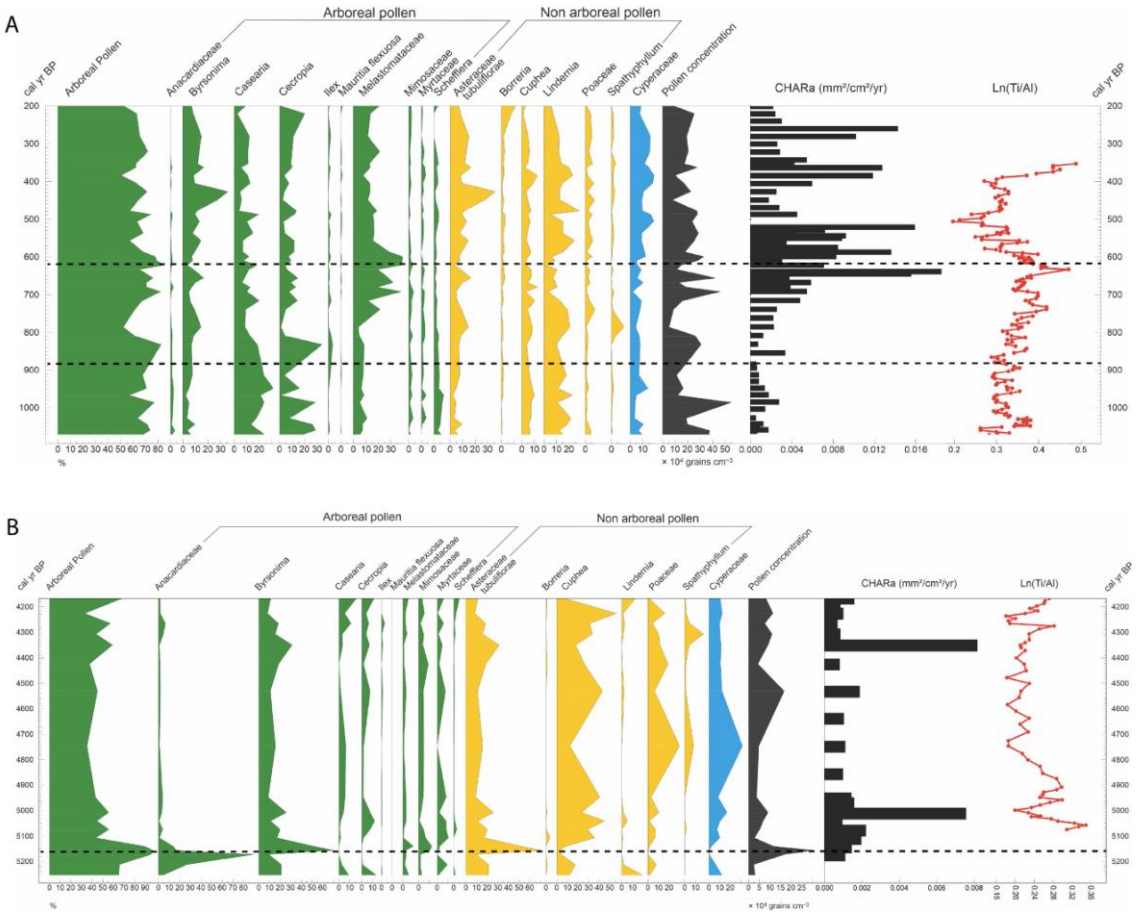

Figure 4. Synthetic diagrams for core OAS-20, showing arboreal pollen (AP) frequency, 17 indicator pollen taxa assigned to arboreal, non-arboreal and water level-related pollen, and geochemical trace element ratios and charcoal area influx (CHARa) represented along a time scale. **(A)** the time interval 1100-200 cal yr BP **(B)** the time interval 5300-4100 cal yr BP. Pollen zones are shown by a dashed line.

For core CHA-20, 65 samples distributed along the 130 cm were taken at 2-cm intervals. Macrocharcoal influx was low (<0.01 mm2/cm2/yr) in the bottom section of the core, but was higher from 3400 cal yr BP (>0.01 mm2/cm2/yr) onward (Fig. 4). The W/L ratio shows a change from mixed fuel to woody particles at ~2000 cal yr BP (Supplementary Figure 9).

289 *Pollen analyses*

290 OAS-20 core

291 Fifty-five samples from 150 cm of core OAS-20 were taken at 2-cm intervals between
292 20 and 170 cm. The resolution of analysis represented on average 60 years per sample
293 in the lower section, and 23 years per sample in the upper section. A total of 118 pollen
294 and spore taxa were identified, comprising 78 arboreal pollen taxa, 28 non-arboreal
295 pollen taxa, two water level-related taxa (*Mauritia* and Cyperaceae) from damp, moist
296 or waterlogged soils) and 10 types of fern spore. The cluster analysis indicated five
297 main intervals of vegetation changes (Supplementary Figure 5), based on the definition
298 of pollen zones described below. The main results are represented along a depth scale
299 and a time scale (Fig. 4 and Supplementary Figure 6).

300 *Pollen zone OAS-1 (167-161cm, 5250-5140 cal yr BP, 5 samples)*

301 Zone OAS-1 (Fig. 4B) was characterized by a high frequency (77%) of arboreal pollen
302 (AP), including *Byrsonima* (20%), *Myracrodruon* (15%), Mimosaceae (6%),
303 Melastomataceae-Combretaceae (6%), *Cecropia* (3%), Myrtaceae (3%) and *Casearia*
304 (3%). A relatively high frequency of non-arboreal pollen (NAP) (19%) included *Cuphea*
305 (9%), *Lindernia* (5%), Poaceae (3%) and Asteraceae (2%). Soil moisture-related taxa
306 were represented by Cyperaceae (100%). Charcoal influx was low (0.1 mm^2/cm^2/year).

307 *Pollen zone OAS-2 (159- 128 cm, 5110 -4170 cal yr BP, 12 samples)*

308 Zone OAS-2 (Fig. 4B) was characterized by a high frequency of NAP (49%) including
309 *Cuphea* (29%), Poaceae (10%), *Asteraceae* (5%), *Spathiphyllum* (4%) and *Lindernia*
310 (1%). A relatively high fequency of AP (39%) included *Byrsonima* (17%), *Myrtaceae*
311 (5%), *Cecropia* (5%), *Casearia* (4%), Mimosaceae (3%), Melastomataceae-
312 Combretaceae (2%), *Myracrodruon* (2%) and *Schefflera* (1%). Soil moisture-related

taxa were represented by Cyperaceae (100%). Charcoal influx fluctuated between 0.8 and 0.06 mm^2/cm^2/year, with two peaks at 152 and 136 cm. Ti/Al levels fluctuated at the base and at the top of the zone.

Pollen zone OAS-3 (126-92 cm, 1100 - 830 cal yr BP, 9 samples)

Zone OAS-3 (Fig. 4A) was characterized by a high frequency of AP (63%) represented by *Casearia* (25%), *Cecropia* (21%), *Byrsonima* (7%), Melastomataceae/Combretaceae (8%), *Schefflera* (5%), Myrtaceae (2%) and Mimosaceae (2%). A relatively high frequency of NAP (29%) included *Lindernia* (18%), *Cuphea* (7%), Asteraceae (3%), Poaceae (2%) and *Spathiphyllum* (1%). Soil moisture-related taxa included Cyperaceae (99%) and, for the first time, the palm tree *Mauritia* (1%). Macrocharcoal influx ranged between 0.2 and 0.06 mm2/ cm^2/year. Ti/Al showed small fluctuations until the end of the zone.

Pollen zone OAS-4 (92- 66 cm, 830- 610 cal yr BP, 12 samples)

Zone OAS-4 (Fig. 4A) was characterized by a high frequency of AP (65%) with Melastomataceae-Combretaceae (25%), *Casearia* (13%), *Cecropia* (11%), *Byrsonima* (10%), Myrtaceae (2%), Mimosaceae (2%) and *Schefflera* (2%). A relatively high frequency of NAP (27%) included *Lindernia* (12%), *Cuphea* (6%), Asteraceae (4%), Poaceae (3%) and *Spathiphyllum* (2%). Soil moisture-related taxa were represented by Cyperaceae (98%) and *Mauritia* (2%). Macrocharcoal influx increased progrressively from 0.01 to 1.8 mm^2/cm^2/yr then decreased at the end of the zone. Ti/Al was relatively stable throughout the zone, until a decrease at the end.

Pollen zone OAS-5 (64-20 cm, 600-200 cal yr BP, 17 samples)

Zone OAS-4 (Fig. 4A) was characterized by a high frequency of AP (56%), including Melastomataceae-Combretaceae (18%), *Byrsonima* (14%), *Casearia* (10%), *Cecropia*

(9%), *Schefflera* (2%), Myrtaceae (1%) and Mimosaceae (2%). NAP frequency reached 30% and included *Lindernia* (15%), *Cuphea* (5%), Asteraceae (5%), Poaceae (4%) and *Spathiphyllum* (1%). Soil moisture-related taxa were represented mainly by Cyperaceae (98%) and *Mauritia* (2%). Charcoal influx fluctuated between 0.1 and 1.5 mm^2/cm^2/year, with no charcoal at ~500 cal yr BP. Ti/Al decreased until the end of the zone, when the trend was inverted.

CHA-20 core

Fifty-seven samples from 118 cm of core CHA-20 were taken at 1-cm intervals between 10 and 128 cm, and were analyzed at 2-cm intervals. The resolution of analysis ranged between 57 and 15 years per sample. A total of 73 pollen taxa, two water level-related taxa (Cyperaceae, Iridaceae and *Xyris*), 10 types of spore and four algae were identified. The cluster analysis indicated five main intervals of vegetation change (Supplementary Figure 7) based on the definition of pollen zones described below. The main results are represented along a time scale in Fig. 5. One tree taxon, *Astronium,* was consistently well represented all along the record with frequency ranging between 2 and 10%.

Pollen zone CHA-1 (128 to 64 cm, 4090 - 2635 cal yr BP, 29 samples)

Zone CHA-1 (Fig. 5) was characterized by 58% AP, with *Ilex* (5%) and *Protium* increasing at the end of the zone, Myrtaceae (1-3%) and absent between 94 and 78 cm (3600 – 2850 cal yr BP), and *Cecropia* (9%), *Curatella* (12%), *Schefflera* (7%). Among the NAP, Poaceae showed the highest frequency (14%), with *Cuphea* being well represented (7%) together with Asteraceae (20%) and Cyperaceae (7%). Macrocharcoal influx appeared in two stages, with a low influx of less than 0.01 mm^2/cm^2/year increasing to 0.04 mm^2/cm^2/year at the end of the zone. Trace elements also occurred in

two stages, with low Ti/Al between 4100 and 3650 cal yr BP, and high Ti/Al between 3650 to 2635 cal yr BP. Ti/Al then abruptly decreased at the end of the zone.

Pollen zone CHA2 (62 to 50 cm, 2560 – 1870 cal yr BP, 9 samples)

Zone CHA-2 (Fig. 5) was characterized by high AP frequencies (66%), including *Ilex* (9%), *Curatella* (5%), *Cecropia* (7%), and *Alchornea* (2%) at the end of the zone. The NAP showed a sharp decrease in Poaceae (0%), and a decrease in Asteraceae (12%) and *Cuphea* (3%), compared with the previous zone, along with Cyperaceae (15%) and *Spathiphyllum* (6%). Macrocharcoal influx was low, ~0.004 mm^2/cm^2/year, at the beginning of thee zone and increased up to 0.075 mm^2/cm^2/year at the end of the zone. After reaching a maximum at ~2400 cal yr BP, Ti/Al decreased progressively until reaching the lowest value of the record at 1890 cal yr BP, synchronous with a charcoal peak.

Pollen zone CHA3 (48 – 30 cm, 1780 – 800 cal yr BP, 10 samples)

Zone CHA-3 (Fig. 5) was characterized by an increase of AP frequencies (84%) and the absence of Poaceae. Among the main tree taxa were observed Melastomataceae-Combretaceae (16%), *Mauritia* (2-11%), *Ilex* (18%), *Alchornea* (3%), *Cecropia* (12%), *Shefflera* (7%), Mimosaceae (3%). NAP was represented by Asteraceae (4%) and Cyperaceae (2%). Macrocharcoal influx fluctuated between 0.05 and 0.2 mm^2/cm^2/year, with a peak of 3.5 mm^2/cm^2/year observed at 1038 cal yr BP. Ti/Al remained stable throughout the zone.

Pollen zone CHA4 (28 – 20 cm, 700 – 250 cal yr BP, 5 samples)

Zone CHA-4 (Fig. 5) was characterized by a small decrease in AP (68%) and the absence of Poaceae. *Curatella* (10%), *Ilex* (6%), *Protium* (4%) and *Mauritia* (17%) were well represented within the AP taxa and *Borreria* (2%) in the NAP. Macrocharcoal

influx was high, ranging between 0.01 and 0.03 mm^2/cm^2/year, and decreasing to 0.003 mm^2/cm^2/year at the end of the zone. Ti/Al levels fluctuated.

Pollen zone CHA5 (18 – 10 cm, 125 – 0 cal yr BP, 5 samples)

Zone CHA-5 (Fig. 5) was characterized by a disappearance of *Protium* and a decrease in *Mauritia* (9%), while *Cecropia* (3%), Melastomataceae-Combretaceae (6%), *Ilex* (1%) and *Astronium* (3%) were well represented. NAP included Asteraceae (7%), and an increase in *Spathiphyllum* (15%), Poaceae (11%), *Borreria* (4%), *Cuphea* (3%) and Cyperaceae (4%). Macrocharcoal influx was low, at 0.003 mm^2/cm^2/year. Ti/Al increased sharply.

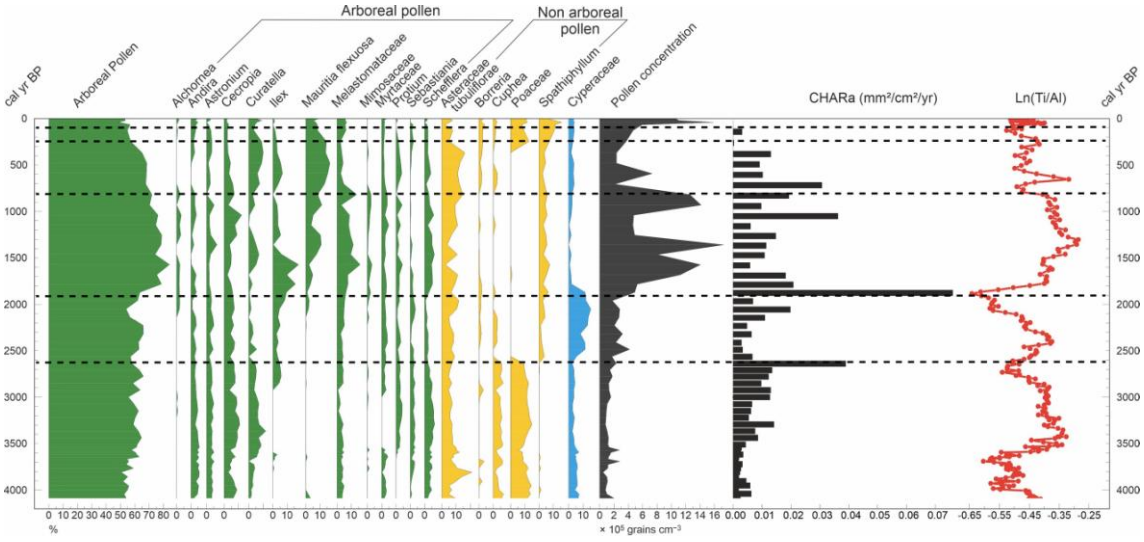

Figure 5. A synthetic diagram for core CHA-20, showing arboreal pollen (AP) frequency, 20 indicator pollen taxa assigned to arboreal, non-arboreal and water level-related pollen, and geochemical trace elements and charcoal area influx (CHARa) represented along a time scale. Pollen zones are shown by a dashed line.

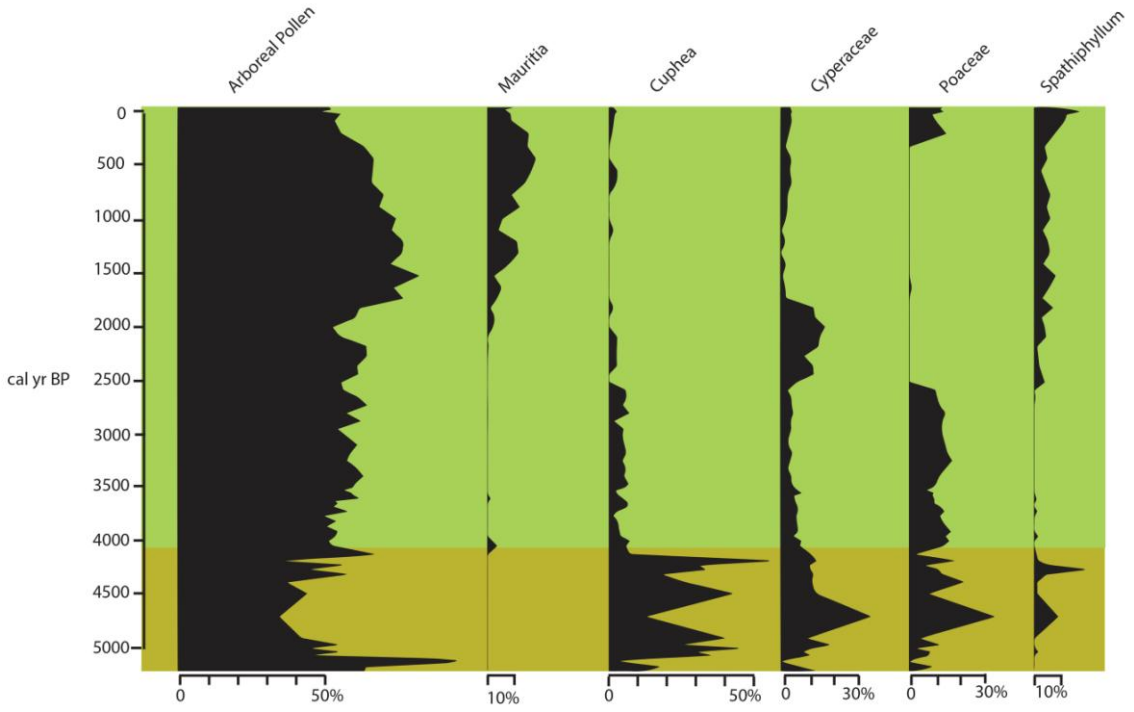

Figure 6. Changes in vegetation at Araripe over the last 5300 years, as reconstructed from changes in arboreal pollen and five indicator taxa from cores OAS-20 (yellow horizontal band between 5300 and 4100 cal yr BP) and CHA-20 (green horizontal band from 4100 cal yr BP to modern).

Interpretation and discussion

Vegetation changes in the region of Araripe

With OAS-20 representing the time intervals 5300 to 4100 cal yr BP and 1100 cal yr BP to present and CHA-20 the interval from 4100 to present, thus covering the hiatus of OAS-20, we reconstructed regional changes in vegetation and fire for the last 5300 years (Fig. 6). Differences in the expression of the vegetation between the two cores for the last 1000 years (the only common interval between the two cores), with higher *Casearia* in OAS-20 and higher *Curatella* in CHA-20s, can probably be explained by their respective locations, with OAS collected in a more humid area (Supplementary Figure 2) and a steeper slope than CHA. For the last 1000 years, our high temporal resolution allowed to compare our changes in vegetation and fire with the climate changes observed by speleothems.

Between 5300 and 4100 cal yr BP, the landscape was open, with a dominance of Poaceae, *Cuphea* and Asteraceae-Tubuliflorae. *Cuphea* is commonly observed today on lake margins around Caatinga or Cerrado (Matias et al., 2021; Ledru et al., 2020). The tree cover was mainly represented by *Byrsonima*, Myrtaceae, and *Piptadenia* (Mimosaceae), species commonly observed today in the Cerrado, Carrasco and Araripe Oasis reserve (Supplemental Table; Benício et al., 2023; Costa and Araújo, 2007). However, their low frequency and concentration suggest that the tree cover was probably scarce and that the area around the aquifer was likely covered by a herbaceous layer including Poaceae, *Cuphea* and Cyperaceae (see Fig. 2). During this interval, fire activity was low, increasing progressively until ~4300 cal yr BP. The charcoal peak at

4300 BP is synchronous with a peak in coarse deposition (Ti/Al; Fig. 4B) which could be due to a single local event.

The hiatus observed in OAS-20 is dated to ~4200 cal yr BP, when a severe drought was observed from western to eastern NEB (Montade et al., 2014; Xavier et al., 2024). CHA-20 sedimentation started at 4100 cal yr BP, and the vegetation represented after the 4200 cal yr BP drought was characterized by tree taxa such as *Astronium*, *Cecropia*, *Schefflera* and *Curatella*, and, among the herbs Asteraceae-Tubuliflorae, *Cuphea*, Poaceae, which suggest a more open landscape with sparse trees of a cerrado until 2700 cal yr BP. Indeed, the tree composition, the persistence of *Cuphea* and the absence of *Spathiphyllum* suggest a dry cerrado similar to the lowland cerrado observed in the region today (Calixto-Júnior et al., 2021), with lower-than-today water levels in the aquifers.

A peak in fire activity was observed between 2700 and 2600 cal yr BP, synchronous with an erosive event (Ti/Al; Fig. 5). The peak could represent a single event with a sudden accumulation of sediment. The interval from 2700 to 2000 cal yr BP was characterized by a change to more humid conditions, with the dry herbaceous layer (*Cuphea*, Poaceae) being replaced by Cyperaceae and the expansion of *Mauritia* and *Ilex* (Fig. 5). The largest peak in fire activity was observed at 2000 cal yr BP and was also synchronous with an erosive event (Ti/Al; Fig. 5). This episode occurred during a gradual change in W/L from a mixed fuel particles towards the dominance of woody particles thus suggesting a sharp change in the landscape.

Between 2000 and 1500 cal yr BP there was a dominance of the moist forest with *Alchornea* and *Ilex*, two indicator taxa for Cerrado gallery forest (Escobar-Torrez et al., 2023a). While at 1500 cal yr BP the dominance of the swamp palm tree *Mauritia* and the herbaceous *Spathiphyllum*, indicates the installation of humid conditions at the

coring sites. *Spathiphyllum* is commonly observed in gallery forest on the river banks (Matias et al., 2021), which in our study area is represented by the aquifer environment.

From 2000 to 1500 cal yr BP the expansion of the moist forest was synchronous with high fire activity, probably the result of local human settlements and activities.

From ~1000 cal yr BP until the last two centuries, *Mauritia* was well represented at Araripe, together with *Ilex* and Melastomataceae-Combretaceae in both records, and *Casearia* in OAS-20, suggesting more humid conditions and higher soil moisture levels. However, this humid interval was interrupted by a drier episode that started at ~900 cal yr BP, including an erosive event indicated by Ti/Al (Fig. 4A and Supplementary Figure 10) followed by an increase in the pioneer taxa *Cecropia* at ~850-800 cal yr BP, with a decrease in regional tree taxa. After 800 cal yr BP, the return of higher moisture levels and high fire activity until ~600 cal yr BP, was observed in both records (Figs 4A and 7). During the last 200 cal yr BP, a decrease in tree taxa including the palm tree *Mauritia flexuosa*, and the re-expansion of Poaceae and an increase in macrocharcoal particles (Figs 6 and 7), can be attributed to an increase in human activities in the Araripe Basin (see below).

Our high temporal resolution results highlight the vulnerability of *Mauritia* in particular, and headwater forest taxa in general, which require permanent edaphic moisture absent during the dry episodes when aquifer water recharge was probably lower.

Climatic implications

Between 5300 and 4200 cal yr BP, the presence of a dry open vegetation at Araripe was anti-phased with the installation of more moist conditions in western NEB (Xavier et al., 2024) and in central Brazil (Escobar Torrez et al., 2023a), when monsoon activity

483 became more intense (Novello et al., 2017). The absence of speleothem deposition at
484 Apodi between 4000 and 3600 cal yr BP was associated with low rainfall, and a dry
485 climate prevailed during the last 4000 years compared with the interval before 5000
486 years ago (Utida et al., 2019). At Araripe, between 4000 and 3000 cal yr BP, the
487 persistence of dry climatic conditions is in agreement with the pollen record from
488 Maranguape, a moist forest refugium ~500 km north of Araripe (Fig. 1B), which
489 showed a drier interval than today from ~5300 to 4200 cal yr BP, and the return of
490 wetter conditions after 3500 cal yr BP (Montade et al., 2014). Thus, the persistence of
491 dry climatic conditions at Araripe after 4000 years suggests that it is located outside the
492 core monsoon domain that reached western NEB during the Holocene (Novello et al.,
493 2017).
494 Headwater forest taxa started to expand after 3000 cal yr BP suggesting moister
495 conditions in the aquifer than during the previous interval, as also indicated by the Ti/Al
496 ratio (Fig. 5 and Supplementary Figure 11), although still drier than during the early-
497 mid Holocene. At the same time, Maranguape and Apodi records (Fig. 1B) showed a
498 return of the forest and an increase in soil production (Montade et al., 2014; Utida et al.,
499 2019). The full expansion of the palm tree *Mauritia* was observed after ~2000 cal yr BP
500 suggesting that the water resource from the aquifer was reduced until at least 2700 cal
501 yr BP. From 3000 cal yr BP onward, the NEB climate shows a dichotomy, with a
502 change from wetter to drier conditions in eastern NEB (Utida et al., 2020), and from
503 drier to wetter conditions in western NEB (Xavier et al., 2024). Our results show that
504 Araripe's climatic evolution synchronized with eastern Brazil, with a wetter pre-4200 yr
505 event (Lima et al., 2021) and a drier climate since then, under the influence of the
506 SASD, winter trade winds and northward cold air incursions (Wainer and Venegas,
507 2002; Wainer et al., 2021).

During the last 1000 years, our high temporal resolution records showed no major changes in the vegetation cover have been observed, suggesting that the aquifer was stable. However, changes in trace elements (Figs 4A and 5) suggest four main variations in the precipitation regime. The first interval, between 1100 and 1000 cal yr BP, is characterized by a high Ti/Al ratio, associated with an increase in coarse sediment and irregular rainfalls. The second interval, between 1000 and 900 cal yr BP, is characterized by a low Ti/Al ratio, associated with fine material and regular rainfall. During the third interval, between 900 and ~500 cal yr BP, the highest Ti/Al ratio in the last 1000 years was seen, with two sharp decreases at 760 cal yr BP and at 600 cal yr BP, corresponding with the dry interval seen at 700-500 cal yr BP at Lake Boqueirão (Utida et al., 2019) and Sete Cidades (Xavier et al., 2022). During this interval an increase in *Curatella*, a tree taxon of the dry cerrado at Araripe (Calixto-Júnior et al., 2021), was observed. Finally, in the fourth interval, between 500 and 350 cal yr BP, the Ti/Al ratio was lower than in the previous interval, in agreement with a relatively humid phase seen at Lake Boqueirão (Utida et al., 2019) and at Sete Cidades (Xavier et al., 2022). In conclusion, the high temporal resolution rainfall variability reconstructed at Araripe for the last 1000 years is in agreement with the results obtained by isotope records and showed an in-phase with the other eastern NEB paleo records.

Fire activity and human impacts

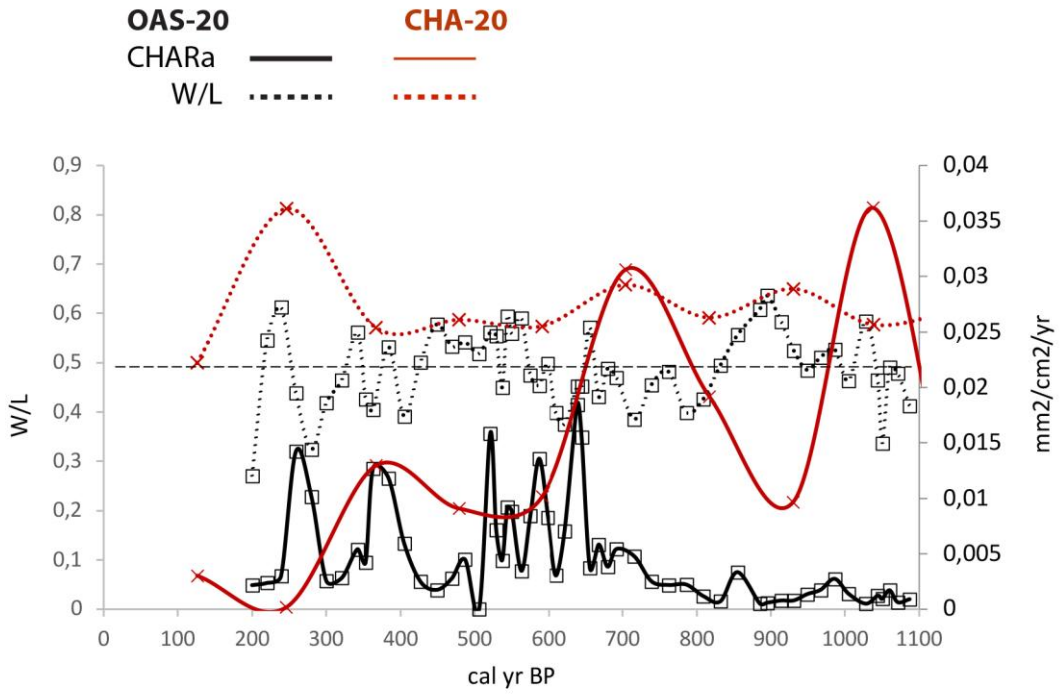

532

533 **Figure 7.** Fire activity at Araripe during the last 1100 years, from cores CHA-20 and OAS-20,
534 based on charcoal influx (CHARa) and the width/length ratio (W/L). The dashed horizontal line
535 shows the 0.5 division used for W/L (see Methods).

536

537 Fire activity at Araripe is similar to other NEB charcoal records deposited in sediment
538 (Oliveira et al., 1999; Moraes et al., 2020; Xavier et al., 2024) (Fig. 1B), with a low
539 influx interrupted by abrupt peaks. The relatively weak fire activity observed in our
540 records is probably related to low ignition (Haliuc et al., 2023). In the earliest part of the
541 OAS-20 record the W/L values less than 0.5 likely characterize the limited availability
542 of fuel in the herbaceous vegetation and the distance between the site and the source of
543 fuel. During the last 4000 years, a dominance of mixed fuel particles is associated to
544 different vegetation and probably some nearby human activity (Haliuc et al., 2023)
545 (Supplementary Figures 8 and 9). The frequency of natural fire regimens is directly
546 related to climate seasonality, and the vegetation type, density and biomass available as
547 a fuel source (Gomes et al., 2018; Pivello et al., 2021). In the Cerrado, natural burnings

occur during the transition from dry to wet seasons, ignited by lightning (Ramos-Neto and Pivello, 2000). The OAS and CHA records showed no increase in CHARa during periods of increased humidity, as for example, at 2700 cal yr BP in CHA-20, where, in contrast, a strong decrease in fire activity was observed (Supplementary Figure 9); or at ~1800 cal yr BP, when a peak in charcoal was associated with erosive conditions and the forest expansion (Figs 5, 6 and Supplementary Figure 11). Thus, charcoal peaks at Araripe are inferred to relate to human activity rather than local natural fire.

During the last 1100 years, the OAS and CHA records show an out-of-phase signal in fire activity, with a higher influx before 650 cal yr BP in CHA-20 and after 650 cal yr BP in OAS-20 (Fig. 7). The last 1100 years are characterized by the presence of the evergreen forest, suggesting that moisture rates were higher than before. In humid forests, natural fires are rare because the high moisture content in the soil and vegetation prevents the biomass burning (Pivello et al., 2021). Thus, the high fire activity observed in our records during the moist phase showed two kinds of origin. First, fires that originated at a distance from our sites, as, for example, the peak observed in the CHA-20 record at 2000 cal yr BP is associated with mixed fuel particles (Fig. 5 and Supplementary Figure 9). Second, fires were locally anthropogenic in character, as, for example, with the absence of a peak in OAS-20 between 500 and 400 cal yr BP associated with woody particles (Fig. 7).

In NEB, the presence of humans dates back 30,000 years (Guidon et al., 1994; Gruhn 2020), and was almost continuous until the mid-Holocene (Bueno, 2011; Herzog, 2017; Lahaye et al., 2015). In the region of Araripe, human settlements relating to Macro-Gê language family, the Kariri group, were recorded during the late Holocene (Souza et al., 2020) until ~340 cal yr BP (1610 AD) (Martin, 2013). The date of 1610 AD could correspond to European arrival also linked to a sharp change in fire activity observed at

both sites between 1350 and 1650 AD (650 and 450 cal yr BP on Fig. 9). Although archaeological information is far too scarce, we suggest that the presence of a water source in the middle of a semi-arid region would have been very attractive for human settlements (Lima-Verde, 2015). Consequently, the observed peaks in macrocharcoal probably relate to an increase in human activities during the last 1100 years at Araripe, with different occupations represented at the two sites.

After 1700 AD, European incursions were seen in the Araripe region, as stockbreeders from the east, searching for new pastures and water resources, started to trade with the native Kariri (Pompeu-Sobrinho, 1956). In the early 1900s, thanks to this exceptional permanent water resource, farmers were able to cultivate sugarcane crops intensively in the middle of the semi-arid, until a decline in the second half of the 20th century (Menezes, 2007). From the 1970s onwards, the abundant and easily accessible water allowed growth of urbanization at Araripe, comprising the cities of Crato, Juazeiro do Norte and Barbalha, is notorious in the context of semi-arid socioeconomic development, popularly known as the “sertão” (Queiroz, 2017).

Today, in arid and semiarid areas managed aquifer recharge (MAR) is often promoted as a solution to water scarcity (Dillon et al., 2022). MAR usually consists in exploiting existing underground storage and negating evaporation losses or climatic changes (Dillon et al., 2022). Our results show that the vegetation is also affected by the changes in the groundwater recharge that strongly relates to rainfall with a percolation time of 180 years for the western region of the plateau and inversely, that this resurgence water also depends on the conservation of the vegetation cover at the plateau. Thus, we show that in a context of recurrent drought, higher temperature and higher evaporation, increasing demand for water for domestic and agricultural consumption, the time of lack of water might come soon, putting a critical threat to the current policies.

Conclusion

Our study highlights the effects of drought and human activity on the diversity and composition of forests and on the water resources of aquifers in Araripe during the last 5300 years. Late Holocene regional changes at Araripe are in phase with eastern NEB climatic pattern with the persistence of drier-than-today climatic conditions after 4000 cal yr BP. The implications of our results are twofold: first, the regional vegetation is associated with global climate changes, e.g., the tree taxon *Curatella*, as an indicator of dry climatic conditions, persisted after the end of the 4200 cal yr BP drought; second, local vegetation at a resurgence e.g., headwater forest taxa, provides an indication of aquifer activity. The aquifers are tightly linked with the mean annual precipitation over the plateau of Araripe, and the current water abundance is a result of the moist phase that has prevailed over the last few centuries. However, with a time lag of ~180 years, along with the projected decreasing of the mean annual rainfall, the amount of water in the aquifers will decrease in the future, thus posing a threat to the water resources. Public policies put in place during the last decade need to be discussed and re-evaluated in the light of our results to ensure future water availability.

Acknowledgements

MDFG is grateful to the “Universidade Regional do Cariri” (URCA) for support and to the “Institut des Sciences de l'Évolution de Montpellier” (ISEM) for hosting her post-doctoral research. We thank the Reserva Particular do Patromônio Natural (RPPN) Oásis Araripe/Aquasis for permission to collect a sediment core, Jean-François Mas for

his assistance during field work, Auriane Mousnier (Master 1 CEPAGE University of Montpellier) for the macrocharcoal analyses of core CHA-20, Sandrine Canal (ISEM) for the macrocharcoal analyses of core OAS-20, and Vivien Mai-Yung-Sen (EDYTEM University of Savoie) for assistance with the XRF scans of the cores.

Funding

This research is part of the projects ANR TASAB "What can a Territory do in the face of the Global Anthropocene Crisis? Socio-environmental Dynamics in the Brazilian Semi-arid" (ANR-22-), and the project JEAI "Le Semi-Aride du Nordeste brésilien à l'Anthropocène" (SANA) at IRD and FUNCAP. It has been funded by the Brazilian National Council of Scientific and Technological Development (CNPq) (grant no 465767/2014-1), the Brazilian Coordination for the Improvement of Higher Education Personnel (CAPES) (grant no 23038.000776/2017-54), and the State of Bahia Research Support Foundation (FAPESB) (grant no INC0006/2019), the support to the National Institute of Science and Technology in Interdisciplinary and Transdisciplinary Studies in Ecology and Evolution (INCT IN-TREE), and the Brazilian Council for Scientific and Technological Development (CNPq) for FSA.

ORCIDs iDs

Maria Daniely Freire Guerra https://orcid.org/0000-0001-5772-9095

Marie-Pierre Ledru https://orcid.org/0000-0002-8079-9320

Sergio Augusto Santos Xavier https://orcid.org/0000-0002-1351-0144

Rudney de Almeida Santos https://orcid.org/0000-0002-1398-1835

Francisca Soares de Araújo https://orcid.org/0000-0003-4661-6137

List of tables

List of figures

669 (B) Evergreen forest, (C) cerradão, (D) cerrado *sensu stricto* and (E) Carrasco (see text for
670 explanation).

671 **Figure 3.** A Bacon age/depth model (red dashed line) for **(A)** core OAS-20 and core **(B)** CHA-
672 20 overlaying the calibrated distributions of the individual radiocarbon dates (blue) (see Tables
673 1 and 2) . Dark gray areas show the 95% confidence intervals of the models (Blaauw and
674 Christen, 2011).

675 **Figure 4.** Synthetic diagrams for core OAS-20, showing arboreal pollen (AP) frequency, 17
676 indicator pollen taxa assigned to arboreal, non-arboreal and water level-related pollen, and
677 geochemical trace element ratios and charcoal area influx (CHARa) represented along a time
678 scale. **(A)** the time interval 1100-200 cal yr BP **(B)** the time interval 5300-4100 cal yr BP.
679 Pollen zones are shown by a dashed line.

680 **Figure 5.** A synthetic diagram for core CHA-20, showing arboreal pollen (AP) frequency, 20
681 indicator pollen taxa assigned to arboreal, non-arboreal and water level-related pollen, and
682 geochemical trace elements and charcoal area influx (CHARa) represented along a time scale.
683 Pollen zones are shown by a dashed line.

684 **Figure 6.** Changes in vegetation at Araripe over the last 5300 years, as reconstructed from
685 changes in arboreal pollen and five indicator taxa from cores OAS-20 (yellow horizontal band
686 between 5300 and 4100 cal yr BP) and CHA-20 (green horizontal band from 4100 cal yr BP to
687 modern).

688 **Figure 7.** Fire activity at Araripe during the last 1100 years, from cores CHA-20 (red line) and
689 OAS-20 (black line), based on charcoal influx (CHARa) and the width/length ratio (W/L)
690 (dotted lines with the same respective colors). The dashed line shows the 0.5 division used for
691 W/L (see Methods).

692

693 ## References

694 Ab'Saber AN (1974) O domínio morfoclimático semi-árido das caatingas brasileiras.

695 *Geomorfologia* 43: 1–39.

696 Aleman JC, Blarquez O, Bentaleb I, et al. (2013) Tracking land-cover changes with
697 sedimentary charcoal in the Afrotropics. *The Holocene* 23(12): 1853–1862. DOI:
698 10.1177/0959683613508159.

699 Alvares CA, Stape JL, Sentelhas PC, et al. (2013) Köppen's climate classification map
700 for Brazil. *Meteorologische Zeitschrift* 22(6): 711–728. DOI: 10.1127/0941-
701 2948/2013/0507.

702 Alves JMB, da Silva EM, Sombra SS, et al. (2017) Eventos extremos diários de chuva
703 no nordeste do Brasil e características atmosféricas. *Revista Brasileira de*
704 *Meteorologia* 32(2): 227–233. DOI: 10.1590/0102-77863220012.

705 Andreoli RV and Kayano MT (2006) Tropical Pacific and South Atlantic effects on
706 rainfall variability over Northeast Brazil. *International Journal of Climatology*
707 26(13): 1895–1912. DOI: 10.1002/joc.1341.

708 Assine ML (2007) Bacia do Araripe. In: *Boletim de Geociencias Da Petrobras*, pp.
709 371–389.

710 Benício RMA, Nascimento A da S, Morais SC de O, et al. (2023) Um refúgio de Mata
711 Úmida no interior do Nordeste brasileiro: estrutura e diversidades alfa e beta.
712 *Ciência Florestal* 33(3): e69097. DOI: 10.5902/1980509869097.

713 Bennett K (2009) Documentation for psimpoll 4.27 and pscomb 1.03. C programs for
714 plotting and analyzing pollen data. Available at:
715 https://chrono.qub.ac.uk/psimpoll/psimpoll.html (accessed 20 November 2022).

716 Blaauw M and Christen JA (2011) Flexible paleoclimate age-depth models using an
717 autoregressive gamma process. *Bayesian Analysis* 6(3): 457–474. DOI:

718 10.1214/11-BA618.

719 Bueno L (2011) L'occupation initiale du Brésil dans une perspective macro-régionale :
720 les cas de l'amazonie, du nordeste et du centre du Brésil. In: Vialou D (ed.)
721 *Peuplements et Préhistoire En Amériques*, pp. 209–220.

722 Bush MB and Weng C (2007) Introducing a new (freeware) tool for palynology.
723 *Journal of Biogeography*. DOI: 10.1111/j.1365-2699.2006.01645.x.

724 Cabral NRAJ and Mota TLN da G (2010) Geoconservacão em áreas protegidas: O caso
725 do geopark araripe - CE. *Natureza a Conservacao* 8(2): 184–186. DOI:
726 10.4322/natcon.00802013.

727 Calixto-Júnior JT, De Moura JC, Lisboa MAN, et al. (2021) Phytosociology, diversity
728 and floristic similarity of a cerrado fragment on southern ceará state, brazilian
729 semiarid. *Scientia Forestalis* 49(130): 1–17. DOI:10.18671/SCIFOR.V49N130.01.

730 Cassino R and Meyer KE (2011) Morfologia de grãos de pólen e esporos de níveis
731 holocênicos de uma vereda do Chapadão dos Gerais (Buritizeiro, Minas Gerais),
732 Brasil. *Gaea - Journal of Geoscience* 7(1): 41–70. DOI: 10.4013/gaea.2011.71.04.

733 Colinvaux P, Oliveira PE and Patiño JEM (1999) *Amazon Pollen Manual and Atlas*. 1st
734 ed. Amsterdam: Harwood Academic Publishers.

735 Costa IR da and Araújo FS de (2007) Organização comunitária de um encrave de
736 cerrado sensu stricto no bioma Caatinga, chapada do Araripe, Barbalha, Ceará.
737 *Acta Botanica Brasilica* 21(2): 281–291. DOI: 10.1590/s0102-
738 33062007000200004.

739 Costa AC, Dupont F, Bler G, et al. (2023) Assessment of aquifer recharge and
740 groundwater availability in a semiarid region of Brazil in the context of an

741 interbasin water transfer scheme. *Hydrogeology Journal* 31:751–769.
742 doi.org/10.1007/s10040-023-02612-x
743 Cruz FW, Vuille M, Burns SJ, et al. (2009) Orbitally driven east-west antiphasing of
744 South American precipitation. *Nature Geoscience* 2(3): 210–214. DOI:
745 10.1038/ngeo444.
746 Dillon, P., W. Alley, Y. Zheng, and J. Vanderzalm (editors), 2022, Managed Aquifer
747 Recharge: Overview and Governance. IAH Special
748 Publication. https://recharge.iah.org/
749 DNPM (1996) Avaliação Hidrogeológica da Bacia Sedimentar do Araripe.
750 *Departamento Nacional da Produção Mineral*. Recife.
751 Escobar-Torrez K, Franco Cassino R and Ledru M-P (2023) Relationship between
752 pollination syndromes, pollen morphology and plant ecology in Quaternary
753 deposits of the Cerrado. *Palynology*: 1–9. DOI: 10.1080/01916122.2023.2252871.
754 Escobar- Torrez K, Ledru M, Cassino RF, et al. (2023) Long- and short- term
755 vegetation change and inferred climate dynamics and anthropogenic activity in the
756 central Cerrado during the Holocene. *Journal of Quaternary Science*: 1–15. DOI:
757 10.1002/jqs.3567.
758 Faegri K and Iversen J (1989) *Textbook of Pollen Analysis*. 4th ed. New York: John
759 Wiley & Sons.
760 FUNCEME (2020) Postos Pluviométricos. Available at:
761 http://www.funceme.br/?page_id=2694.
762 FUNCEME (2021) Chove em cerca de 60 municípios; Crato acumula 111 mm em 24
763 horas. Available at: http://www.funceme.br/?p=9853.

764 FUNCEME (2023) Índices de aridez do Estado do Ceará. Available at:
765 http://www.funceme.br/?page_id=5826.

766 Gomes L, Miranda HS and Bustamante MM da C (2018) How can we advance the
767 knowledge on the behavior and effects of fire in the Cerrado biome? *Forest*
768 *Ecology and Management* 417: 281–290. DOI: 10.1016/j.foreco.2018.02.032.

769 Grimm EC (1987) CONISS: a FORTRAN 77 program for stratigraphically constrained
770 cluster analysis by the method of incremental sum of squares. *Computers and*
771 *Geosciences* 13(1): 13–35. DOI: 10.1016/0098-3004(87)90022-7.

772 Gruhn R (2020) Evidence growing fo early peopling of the Americas. *Nature* 584: 47-
773 48.

774 Guerra MDF, Souza MJN and Silva E V. (2020) Palm swamps of the Araripe Plateau:
775 subspaces of exception in the semiarid of the state of Ceará, Brazil. *Ateliê*
776 *Geográfico* 14(2): 51–66.

777 Guerra MDF, Lelis Leal de Souza JJ, Gonçalves Reynaud Schaefer CE, et al. (2023)
778 Remnant wetlands under palm swamps in the Araripe Plateau, Brazilian semiarid.
779 *Catena* 226: 1–5. DOI: 10.1016/j.catena.2023.107074.

780 Guidon N, Parenti F, Da Luz M de F, et al. (1994) Le plus ancien peuplement de
781 l'Amérique : le Paléolithique du Nordeste brésilien. *Bulletin de la Société*
782 *préhistorique française* 91(4): 246–250. DOI: 10.3406/bspf.1994.9732.

783 Haliuc, A., Daniau, A.-L., Mouillot, F., et al (2023) Microscopic charcoals in
784 ocean sediments off Africa track past fire intensity from the continent.
785 *Communications Earth & Environment* 4: 1e11v.

786 Herzog A (2017) Paisagens Geológicas e Geoparques: o Geoparque Araripe. In:

Mongelli MM and Castriota LB (eds) *1º Colóquio Ibero-Americano Paisagem Cultural, Patrimônio e Projeto*. IPHAN, pp. 420–435.

Hogg AG, Heaton TJ, Hua Q, et al. (2020) SHCal20 Southern Hemisphere Calibration, 0-55,000 Years cal BP. *Radiocarbon* 62(4): 759–778. DOI: 10.1017/RDC.2020.59.

Lahaye C, Guérin G, Boëda E, et al. (2015) New insights into a late-Pleistocene human occupation in America: The Vale da Pedra Furada complete chronological study. *Quaternary Geochronology* 30: 445–451. DOI: 10.1016/j.quageo.2015.03.009.

Ledru MP and Araújo FS (2023) The Cerrado and restinga pathways: two ancient biotic corridors in the neotropics. *Frontiers of Biogeography* 15(3): e59398. DOI: 10.21425/F5FBG59398.

Ledru MP, Jeske-Pieruschka V, Bremond L, et al. (2020) When archives are missing, deciphering the effects of public policies and climate variability on the Brazilian semi-arid region using sediment core studies. *Science of the Total Environment* 723. DOI: 10.1016/j.scitotenv.2020.137989.

Lemos JR and Meguro M (2015) Estudo fitossociológico de uma área de Caatinga na Estação Ecológica (ESEC) de Aiuaba, Ceará, Brasil. *Biotemas* 28(2): 39. DOI: 10.5007/2175-7925.2015v28n2p39.

Lima-Verde R (2015) *Arqueologia social inclusiva: a Fundação Casa Grande e a gestão do patrimônio cultural da Chapada do Araripe, Nova Olinda, CE, Brasil*. Tese de doutorado. Universidade de Coimbra.

Lima GG, Marçal M, de Barros Correa AC, et al. (2021) Landscape evolution of the Salamanca watershed, Araripe Plateau: Insights from a river channel morphological classification. *Journal of South American Earth Sciences* 107:

103013. DOI: 10.1016/j.jsames.2020.103013.

Loiola MIB, Araújo FS, Lima-Verde LW, et al. (2015) Flora da Chapada do Araripe. In: *Sociobiodiversidade Na Chapada Do Araripe*, pp. 103–148.

Lorente FL, Buso Junior AA, Oliveira PE de, et al. (2017) *Atlas Palinológico: Laboratório 14C/USP*. Piracicaba, SP: FEALQ.

Macêdo MS (2014) *Análise estrutural da vegetação de cerradão em áreas conservada e em regeneração no Nordeste do Brasil*. Dissertação de mestrado. Universidade Regional do Cariri, URCA.

Machado CJF, Santiago MMF, Mendonça LAR, et al. (2007) Hydrogeochemical and flow modeling of aquitard percolation in the Cariri Valley-Northeast Brazil. *Aquatic Geochemistry* 13(2): 187–196. DOI: 10.1007/s10498-007-9015-y.

Marengo JA and Bernasconi M (2015) Regional differences in aridity/drought conditions over Northeast Brazil: present state and future projections. *Climatic Change* 129(1–2): 103–115. DOI: 10.1007/s10584-014-1310-1.

Marengo JA, Liebmann B, Grimm AM, et al. (2012) Recent developments on the South American monsoon system. *International Journal of Climatology*. DOI: 10.1002/joc.2254.

Marengo JA, Alves LM, Alvala RCS, et al. (2018) Climatic characteristics of the 2010-2016 drought in the semiarid northeast Brazil region. *Anais da Academia Brasileira de Ciencias* 90(2): 1973–1985. DOI: 10.1590/0001-3765201720170206.

Marengo JA, Cunha APMA, Nobre CA, et al. (2020) Assessing drought in the drylands of northeast Brazil under regional warming exceeding 4 °C. *Natural Hazards* 103(2): 2589–2611. DOI: 10.1007/s11069-020-04097-3.

833 Marengo JA, Galdos MV, Challinor A, et al. (2022) Drought in Northeast Brazil: A
834 review of agricultural andpolicy adaptation options for food security. *Climate*
835 *Resilience and Sustainability* doi.org/10.1002/cli2.17
836
837 Martin G (2013) *Pré-História Do Nordeste Do Brasil*. 5th ed. Recife: Editora
838 Universitária da UFPE.
839 Matias LQ, Guedes FM, Do Nascimento HP, et al. (2021) Breaking the misconception
840 of a dry and lifeless semiarid region: The diversity and distribution of aquatic flora
841 in wetlands of the brazilian northeast. *Acta Botanica Brasilica* 35(1): 46–61. DOI:
842 10.1590/0102-33062020ABB0236.
843 Mendonça LAR (2001) *Recursos hídricos da Chapada do Araripe*. Tese de doutorado.
844 Universidade Federal do Ceará.
845 Mendonça LAR, Frischkorn H, Santiago MMF, et al. (2004) Probing the relationship
846 between surface waters and aquifers by ^{18}O measurements on the top of the Araripe
847 Plateau/NE Brazil. *Environmental Earth Sciences* 46(2):295-302.
848 DOI:10.1007/s00254-004-0975-6
849 Menezes EO (2007) O Cariri cearense. In: Borzacchiello J, Cavalcante T, and Dantas E
850 (eds) *Ceará: Um Novo Olhar Geográfico*. Fortaleza, pp. 339–363.
851 Montade V, Ledru MP, Burte J, et al. (2014) Stability of a neotropical microrefugium
852 during climatic instability. *Journal of Biogeography* 41(6): 1215–1226. DOI:
853 10.1111/jbi.12283.
854 Montade V, Diogo IJS, Bremond L, et al. (2016) Pollen-based characterization of
855 montane forest types in north-eastern Brazil. *Review of Palaeobotany and*
856 *Palynology* 234: 147–158. DOI: 10.1016/j.revpalbo.2016.07.003.

857 Moraes CA de, de Oliveira MAT and Behling H (2020) Late Holocene climate
858 dynamics and human impact inferred from vegetation and fire history of the
859 Caatinga, in Northeast Brazil. *Review of Palaeobotany and Palynology* 282:
860 104299. DOI: 10.1016/j.revpalbo.2020.104299.

861 Morales N and Assine ML (2015) Chapada Do Araripe: A Highland Oasis Incrusted
862 into the Semi-arid Region of Northeastern Brazil. In: *World Geomorphological*
863 *Landscapes*, pp. 231–242. DOI: 10.1007/978-94-017-8023-0_21.

864 Moro MF, Macedo MB, De Moura-Fè MM, et al. (2015) Vegetation, phytoecological
865 regions and landscape diversity in Ceará state, northeastern Brazil. *Rodriguesia*
866 66(3): 717–743. DOI: 10.1590/2175-7860201566305.

867 Moro MF, Nic Lughadha E, de Araújo FS, et al. (2016) A Phytogeographical
868 Metaanalysis of the Semiarid Caatinga Domain in Brazil. *Botanical Review* 82(2):
869 91–148. DOI: 10.1007/s12229-016-9164-z.

870 Nimer E (1989) Climatologia da Região Nordeste. In: *Climatologia Do Brasil*. 2nd ed.
871 Rio de Janeiro: IBGE, pp. 315–362.

872 Novello VF, Cruz FW, Vuille M, et al. (2017) A high-resolution history of the South
873 American Monsoon from Last Glacial Maximum to the Holocene. *Scientific*
874 *Reports* 7. DOI: 10.1038/srep44267.

875 Oliveira PE, Magnólia A, Barreto F, et al. (1999) Late Pleistocene/Holocene climatic
876 and vegetational history of the Brazilian caatinga: the fossil dunes of the middle
877 São Francisco River. *Palaeogeography, Palaeoclimatology, Palaeoecology* 152:
878 319–337.

879 Pivello VR, Vieira I, Christianini A V., et al. (2021) Understanding Brazil's

880 catastrophic fires: Causes, consequences and policy needed to prevent future
881 tragedies. *Perspectives in Ecology and Conservation* 19(3): 233–255. DOI:
882 10.1016/j.pecon.2021.06.005.

883 Pompeu-Sobrinho T (1956) O povoamento do Cariri cearense. *Revista da Acadêmia*
884 *Cearense de Letras* 27: 195–205.

885 Queiroz I da S (2017) A emergência da região metropolitana do Cariri cearense no
886 âmbito estadual e dos sertões centrais do Nordeste. In: Pinheiro VF, Alves CLB,
887 Lima-Júnior FO, et al. (eds) *Para Pensar o Desenvolvimento Da RM Cariri*. São
888 Paulo: Blucher, pp. 51–67.

889 Ramos-Neto MB and Pivello VR (2000) Lightning fires in a Brazilian Savanna National
890 Park: Rethinking management strategies. *Environmental Management* 26(6): 675–
891 684. DOI: 10.1007/s002670010124.

892 Rao VB, de Lima MC and Franchito SH (1993) Seasonal and Interannual Variations of
893 Rainfall over Eastern Northeast Brazil. *Journal of Climate* 6(9): 1754–1763. DOI:
894 10.1175/1520-0442(1993)006<1754:SAIVOR>2.0.CO;2.

895 Ratter JA, Bridgewater S and Ribeiro JF (2003) Analysis of the floristic composition of
896 the Brazilian Cerrado vegetation III: comparison of the woody vegetation of 376
897 areas. *Edinburgh Journal of Botany* 60(1): 57–109.
898 DOI:10.10M/S0960428603000064.

899 Ribeiro-Silva S, Medeiros MB De, Gomes BM, et al. (2012) Angiosperms from the
900 Araripe National Forest, Ceará, Brazil. *Check List* 8(4): 744–751.

901 Sampaio EVSB (1995) Overview of the Brazilian Caatinga. In: Bullock S, Mooney HA,
902 Medina E (eds) *Seasonally Dry Tropical Forests*. Cambridge University Press:

New York, pp. 35–58.

Santiago MF, Silva CMS V., Filho JM, et al. (1997) Characterization of Groundwater in the Cariri (Ceará, Brazil) By Environmental Isotopes and Electric Conductivity. *Radiocarbon* 39(1): 49–59. DOI: 10.1017/S0033822200040893.

Santos JEG dos, Bezerra JWA, Silva VB da, et al. (2019) Phytosociology a Humid Forest of the Chapada of Araripe, Crato, CE, Brazil. *Journal of Agricultural Science* 11(7): 115. DOI: 10.5539/jas.v11n7p115.

Santos R de A and Ledru MP (2021) Acid-free protocol for extracting pollen from Quaternary sediments. *Palynology* 46: 1–8. DOI:10.1080/01916122.2021.1960916.

Silveira MHB, Mascarenhas R, Cardoso D, et al. (2019) Pleistocene climatic instability drove the historical distribution of forest islands in the northeastern Brazilian Atlantic Forest. *Palaeogeography, Palaeoclimatology, Palaeoecology* 527: 67–76. DOI: 10.1016/j.palaeo.2019.04.028.

Souza JG de, Mateos JA and Madella M (2020) Archaeological expansions in tropical South America during the late Holocene: Assessing the role of demic diffusion. *PLoS ONE* 15(4). DOI: 10.1371/journal.pone.0232367.

Stevenson J and Haberle S (2005) *Macro Charcoal Analysis: A Modified Technique Used by the Department of Archaeology and Natural History*.

Stockmarr J (1971) Tablets with Spores Used in Absolute Pollen Analysis. *Pollen et Spores* 13: 615-621.

SUDENE (1975) Rede hidroclimatológica do Nordeste. Available at: http://www.sudene.gov.br/area-de-atuacao/regiao-nordeste-estatisticas/rede-hidroclimatologica-do-nordeste.

926 SUDENE (2017) Resolução N^{o} 115, de 23 de Novembro de 2017. Available at:
927 https://www.ibge.gov.br/geociencias/cartas-e-mapas/mapas-regionais/15974-
928 semiarido-brasileiro.html?=&t=downloads.

929 SUDENE (2021) *Delimitação do semiárido. Superintendência do Desenvolvimento do*
930 *Nordeste*. Recife.

931 Utida G, Cruz FW, Etourneau J, et al. (2019) Tropical South Atlantic influence on
932 Northeastern Brazil precipitation and ITCZ displacement during the past 2300
933 years. *Scientific Reports* 9(1). DOI: 10.1038/s41598-018-38003-6.

934 Utida G, Cruz FW, Santos R V., et al. (2020) Climate changes in Northeastern Brazil
935 from deglacial to Meghalayan periods and related environmental impacts.
936 *Quaternary Science Reviews* 250. DOI: 10.1016/j.quascirev.2020.106655.

937 Wainer I and Venegas SA (2002) South Atlantic multidecadal variability in the climate
938 system model. *Journal of Climate* 15(12): 1408–1420. DOI: 10.1175/1520-
939 0442(2002)015<1408:SAMVIT>2.0.CO;2.

940 Wainer I, Prado LF, Khodri M, et al. (2021) The South Atlantic sub-tropical dipole
941 mode since the last deglaciation and changes in rainfall. *Climate Dynamics* 56(1–
942 2): 109–122. DOI: 10.1007/s00382-020-05468-z.

943 Xavier SAS, Araújo FS de and Ledru MP (2022) Changes in fire activity and
944 biodiversity in a Northeast Brazilian Cerrado over the last 800 years. *Anthropocene*
945 40, 100356. doi.org/10.1016/j.ancene.2022.100356. .

946 Xavier SAS, Ledru MP, Bremond L, et al. (2024) Millennial-scale variability of
947 vegetation and fire activity in a northern Cerrado driven by an east-west rainfall
948 gradient during the Holocene. *The Holocene* DOI: 10.1177/09596836231225719.

949